Edge Thermal Transport Barrier In LHD Discharges

N. Ohyabu, K. Narihara, H. Funaba, T. Morisaki, S. Masuzaki, K. Kawahata, A. Komori, O. Kaneko, H. Yamada, P. deVries, M. Emoto, M. Goto, Y. Hamada, K. Ida, H. Idei, S. Inagaki, N. Inoue, S. Kado, S. Kubo, R. Kumazawa, T. Minami, J. Miyazawa, S. Morita, S. Murakami, T. Mutoh, S. Muto, Y. Nagayama, Y. Nakamura, H. Nakanishi, K. Nishimura, N. Noda, T. Kobuchi, S. Ohdachi, K. Ohkubo, Y. Oka, M. Osakabe, T. Ozaki, B. J. Peterson, A. Sagara, S. Sakakibara, R. Sakamoto, H. Sasao, M. Sasao, K. Sato, K. Saito, M. Sato, T. Seki, T. Shimozuma, M. Shoji, H. Suzuki, S. Sudo, Y. Takeiri, K. Tanaka, K. Toi, T. Tokuzawa, K. Tsumori, K. Tsuzuki, I. Yamada, S. Yamaguchi, K. Yamazaki, M. Yokoyama, K. Y. Watanabe, T. Watari, and O. Motojima

National Institute for Fusion Science, Toki, Gifu-ken, Japan

(Received 13 May 1999)

In LHD discharges a significant enhancement of the global energy confinement has been achieved for the first time in a helical device with an edge thermal barrier, which exhibits a sharp gradient at the edge of the temperature profile. Key features associated with the barrier are quite different from those seen in tokamaks: (i) almost no change in particle (including impurity) transport, (ii) a gradual formation of the barrier, (iii) a very high ratio of the edge temperature to the average temperature, and (iv) no edge relaxation phenomenon. These features are very attractive in applying the thermal barrier to future reactor grade devices.

PACS numbers: 52.55.Hc

The Large Helical Device (LHD) is a new large heliotron type device with a divertor [$l = 2$, $m = 10$, $R_{\rm ax}$ (position of magnetic axis) = 3.6–3.9 m, a (minor radius) = 0.6 m, $B = 3$ T] [1]. The major goal of the LHD experiment is to demonstrate high performance of a helical plasma in a reactor relevant plasma regime. In tokamak research, the so-called H mode was discovered in 1982 [2], in which the edge thermal barrier enhances the confinement by a factor of up to 2. We have achieved a significant enhancement of the global energy confinement with an edge thermal barrier. However, the key observed features of the LHD barrier are quite different from those seen in tokamaks [2,3] and are very favorable and attractive for applying it to reactor grade devices. In smaller helical devices, edge transport barrier (H mode) [4,5] and internal electron transport barrier [6] have also been observed. But enhancement of the global energy confinement, however, is minimal, $\sim$30%.

We have observed a high edge temperature plasma, which is similar to the edge temperature pedestal, generated by the H-mode edge thermal transport barrier [2,3]. Figure 1 shows the temperature profile during the flat top of a typical LHD discharge. This profile is measured by Thomson scattering along the major radius (R) ($Z = 0$) at the poloidal plane where the plasma is elongated horizontally [Fig. 1(b)]. In Fig. 1(a), T_e is plotted as a function of R. A mild pedestal with a shoulder temperature ($T_e^{\rm ped}$) of $\sim$500 eV can be seen. In the outer region ($2.8 < R < 3.0$ m and $4.4 < R < 4.7$ m) where the pedestal exists, the flux surface is expanded toward the X points significantly [Fig. 1(b)]. Thus it may be more appropriate to plot it as a function of ρ (normalized effective radius) with an assumption that T_e is constant on the flux surface [Fig. 1(c)]. In this plot, much sharper T_e gradient at the edge appears. The estimated total thermal conductivity ($n_c\chi$) there is fairly low, typically $\sim 2.0 \times 10^{19}$ m^{-1} s^{-1} and thus transport in this edge region can be called edge thermal transport barrier. Here we assume that $T_e(r) = T_i(r)$ (the ion temperature). Our T_i profile measurement is very limited at this moment. The T_i profile in the region $0.3 < \rho < 0.9$ for the low density discharges is found to be close to that of T_e. From a flux surface mapping of the T_e profile, the width of the pedestal is $\sim$4 cm in the Z direction ($\sim$0.10 in ρ), which appears to be much larger than the poloidal ion gyroradius (1.5 cm). The maximum shoulder temperature ($T_e^{\rm ped}$) obtained to date is 1.2 keV.

The LHD edge magnetic structure is complicated [7], as illustrated in Fig. 2(a). An ergodic region exists beyond the last closed magnetic surface (LCMS, i.e., $\rho = 1$ surface). It is generated by island layers with toroidal mode number of 10. The connection length L_c (the field line length to the divertor plates) is $>$1000 m. Beyond this region, there exists a more open region with multiple thin edge surface layers which corresponds to the spikes of the L_c in Fig. 2(b). The field lines between the layers connect the divertor plate at one location to the plate at the other location in a short distance. The temperature is low (below 40 eV) in the multiple surface layer region. On the other hand, a significant density gradient exists there and the density at $R = 4.66$ m, where T_e starts to rise, is $\sim$50% of the shoulder density, which is close to the average density. This means that particle confinement almost takes place in the edge surface layer region. This is not surprising since cold ions are well confined in the open edge region where the connection length is longer than $\sim$300 m. In the ergodic region ($4.60 < R < 4.66$ m), the temperature increases modestly from 40 eV at $R = 4.66$ m to 80 eV

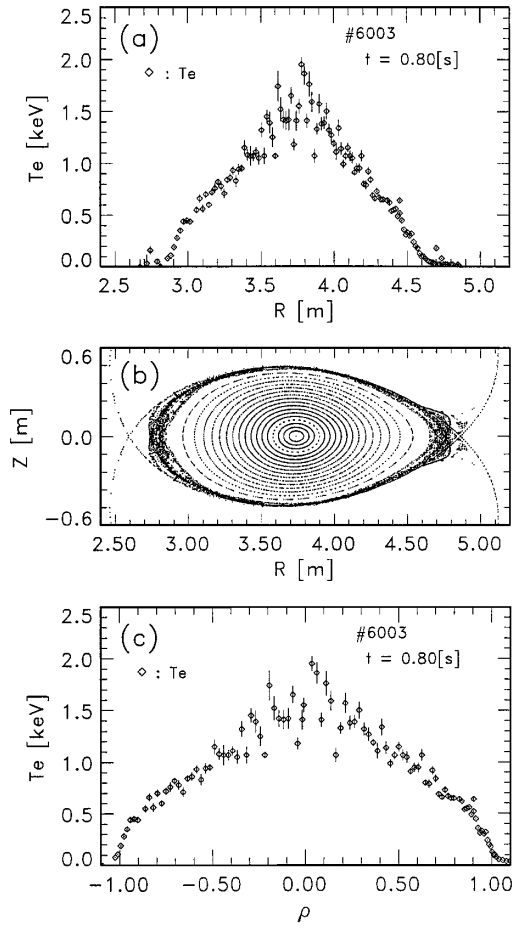

FIG. 1. (a) A typical electron temperature profile [$R_{\rm ax} = 3.70$ m, $B = 1.5$ T, n_e (the line average density) $= 2.2 \times 10^{19}$ m^{-3}] measured by Thomson scattering. A pedestal, i.e., high ∇T_c region, is seen in the edge. (b) The LHD magnetic configuration. The T_e profile is measured along the major radius (R axis) ($Z = 0$). (c) The electron temperature profile is plotted as a function of ρ. The data points with negative value of ρ are from those in the inner region ($R < 3.75$ m) in (a).

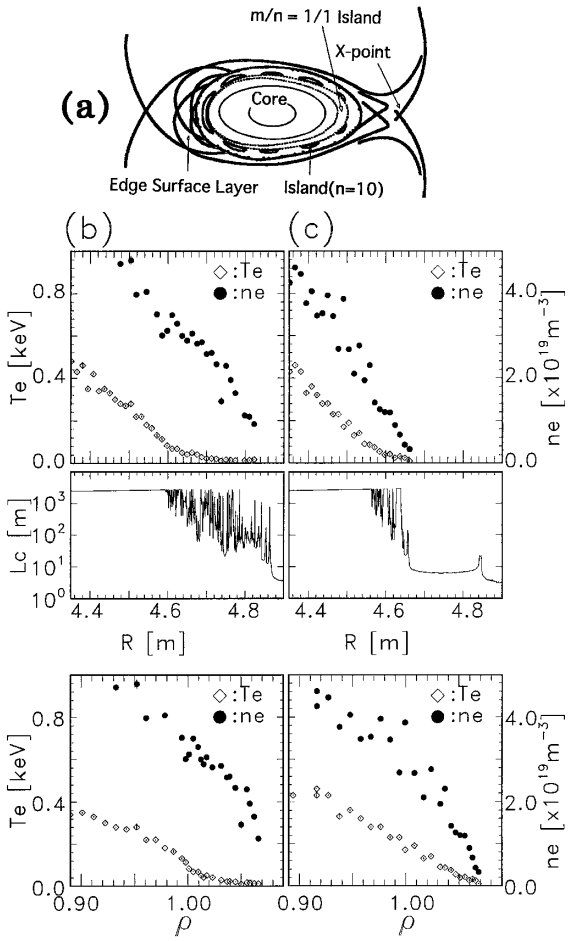

FIG. 2. (a) An illustration of the LHD edge magnetic structure. (b) T_e and n_e profiles, the connection length (L_c) in the edge region for the discharge with $R_{\rm ax} = 3.70$ m and $B = 1.5$ T. (c) Edge profiles for the discharge with $R_{\rm ax} = 3.60$ m and $B = 2.75$ T.

at $R = 4.60$ m ($\rho = 1$). For the inward shifted configuration [$R_{\rm ax} = 3.60$ m, Fig. 2(c)], the ergodic and multiple curved layer regions are much narrower. This results in a fair overlapping of the high ∇T_e and high ∇n_e regions, which is believed to be a favorable condition for the confinement enhancement. Indeed this configuration exhibits a factor of $\sim$25% improvement of τ_E over the configurations with larger $R_{\rm ax}$ ($= 3.70$ m).

In the H-mode discharges, the edge confinement suddenly improves after a so-called L-H transition, forming the temperature and density pedestals. The pedestal in the LHD discharge forms during the rising phase, not through a rapid transition. Figure 3 shows temporal evolution of the LHD discharge. At 400 msec, a neutral beam (3.5 MW) injected into a small target plasma discharge generated by electron-cyclotron heating. With beam heating on, the hot plasma region expands radially and eventually reaches the LCMS and divertor plates, evidenced by an increase in the ion saturation current ($\Gamma_{\rm div}$) measured by the probes at the inner divertor strike points. At the same time, $T_e^{\rm ped}$ [temperature at $\rho = 0.9$ ($R = 4.40$ m)] increases rapidly to 250 eV. At $t = 600$ ms, the gas puff is turned off and 100 ms later, the density starts to decrease. But W_p increases by $\sim$30% accompanied by a substantial increase in $T_e^{\rm ped}$. Unlike in the conventional H-mode discharges, the density and the total radiation power ($P_{\rm rad}$) are maintained fairly constant in the LHD discharges.

In Fig. 4, we plot the stored energy (W_p), the central, average, and pedestal temperatures, particle flux as a function of n_e. In this series of shots, neutral-beam injection (NBI) power (3.5 MW) is injected into discharges ($B = 1.5$ T, $R_{\rm ax} = 3.70$ m) with various average densities. The edge temperature decreases gradually with the average density. This may be related to a gradual increase in the recycling flux [ion saturation current at the divertor ($\Gamma_{\rm div}$) and helium neutral pressure in the vessel ($P_{\rm He}$)] with n_e. The pedestal temperature is found to be very close to the average temperature ($\langle T_e \rangle$) ($T_e^{\rm ped}/\langle T_e \rangle$ is as high as 0.7–0.8).

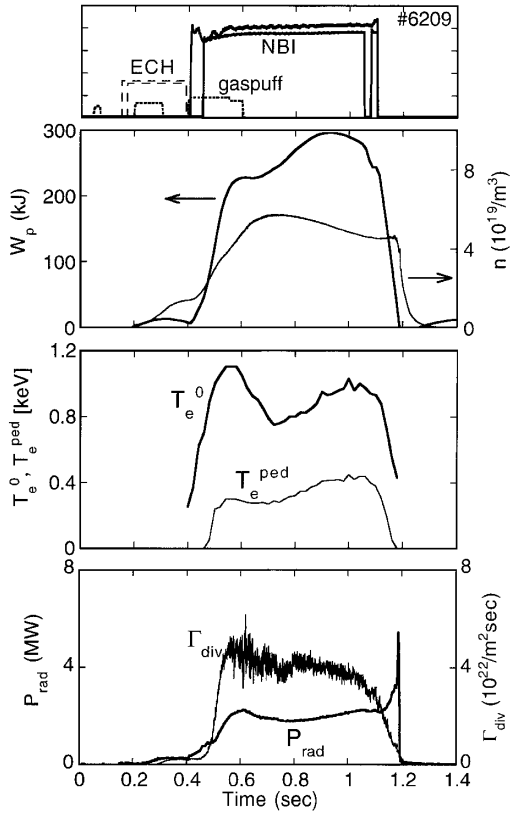

FIG. 3. Temporal evolution of a typical LHD discharge. W_p is the total stored plasma energy. $\Gamma_{\rm div}$ is from ion saturation current measurement at an inner strike point of the divertor leg. $P_{\rm rad}$ is the total radiation power measured by a bolometric system.

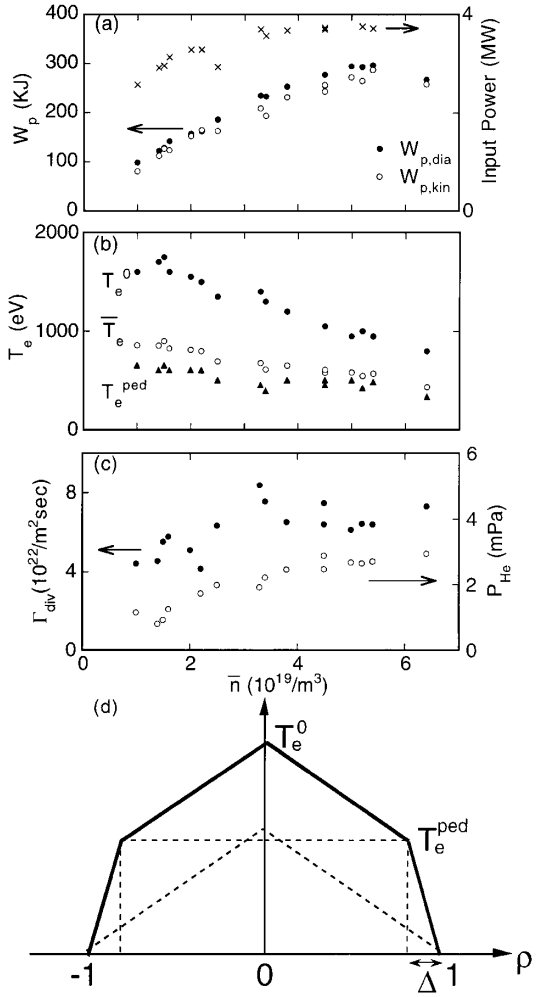

FIG. 4. Dependence of W_p, T_e^0, $\langle T_e\rangle$, $T_e^{\rm ped}$, $\Gamma_{\rm div}$, and $P_{\rm He}$ on n_e with $B = 1.5$ T, $R_{\rm ax} = 3.70$ m, helium plasma. T_e^0: the central electron temperature, $T_e^{\rm ped}$: the pedestal electron temperature, $\langle T_e\rangle$: the average electron temperature, $P_{\rm He}$: the helium neutral pressure measured by fast ionization gauge. (d) A model T_e profile for LHD discharges. A profile shown by dotted lines is a hypothetical one without pedestal.

Most of the T_e profiles in the LHD discharges can be approximated by a simplified model profile depicted in Fig. 4(d). In this model profile with normalized width (Δ) of $4/45$, the average temperature ($\langle T_e\rangle$) is given by

$$\langle T_e\rangle = 0.91T_e^{\rm ped} + 0.28(T_e^0 - T_e^{\rm ped}). \qquad (1)$$

In Fig. 4(a), the stored plasma energy ($W_{p,\rm dia}$) measured by diamagnetic loop and the stored plasma energy ($W_{p,\rm kin} = 1.5 \times \frac{3}{2} n_e\langle T_e\rangle V$) are plotted as a function of n_e. Here V is the volume of the plasma (26 m^3), and $\langle T_e\rangle$ is estimated by the above Eq. (1) and measured values of T_e^0, $T_e^{\rm ped}$. A factor of 1.5 comes from an assumption that $T_e(\rho) = T_i(\rho)$ for the helium discharges. Nearly perfect agreement between the two parameters shows the validity of the model temperature profile. For the present LHD plasmas, the first term in Eq. (1) is much greater than the second term, i.e., W_p is nearly proportional to $n_e T_e^{\rm ped}$. For the H-mode cases, enhancement of τ_E can be easily estimated by comparing the stored energies just before and well after the H transition. For the LHD discharges, which do not exhibit any transition, we consider a hypothetical T_e profile with the same $\partial T_e/\partial r$ as that observed in the core, but without pedestal, as shown by dotted lines in Fig. 4(d). By comparing real and hypothetical profiles, we find that enhancement factor of τ_E is between 2 and 3 for the discharges in Fig. 4. This is a significant enhancement. Such a comparison is justified from experimental observations, e.g., when excessive gas puffing or impurity puffing cools the edge, the profile approaches one similar to the hypothetical one with a substantial reduction of τ_E. We have studied configurations with different position of the axis ($R_{\rm ax}$) from 3.6 to 3.9 m and for the inward shifted configuration ($R_{\rm ax} = 3.6$ m) with good particle orbit properties exhibits a factor of 1.5 enhancement over the ISS95 (International Stellerator Scaling) [8]. The enhancement factor appears to decrease with increasing $R_{\rm ax}$. Compared with the empirical scaling based on heliotron type smaller devices (which is $\sim$30% lower than the ISS95), the enhancement factor is $\sim$2. The

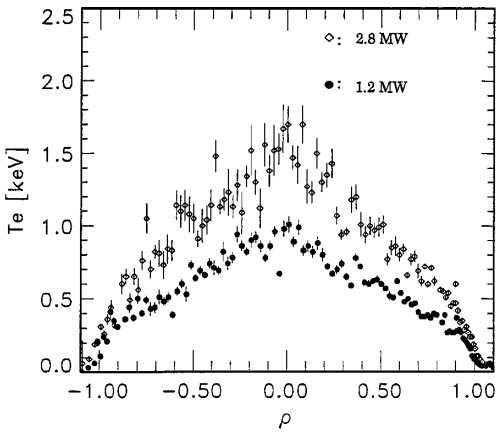

FIG. 5. Variation of electron temperature profile for different levels of injected NBI power.

enhancement over the scalings is believed to be due to the edge transport barrier.

Figure 5 shows T_e profiles at different input power levels. The other parameters are the same ($n_e = 2.5 \times 10^{19}$ m^{-3}, $B = 1.5$ T, $R_{\rm ax} = 3.70$ m). The values of ∇T_e at the pedestal are nearly the same, but the width of the pedestal appears to be much wider for the high power case. The edge temperature and density at the pedestal shoulder are comparable to those of the comparable tokamaks, but the edge pressure gradient is lower due to wider pedestal width. The normalized pressure gradient defined as $\nabla p_N = a\nabla P/(B^2/2\mu)$ is still as high as 0.06 at the middle of the steep gradient, which is close to the Mercier stability limit. In the tokamak H mode, edge localized modes (ELMs) appear repetitively, expelling a fraction of the particle and energy to the divertor plates in a short time. It has been argued that an ELM is a MHD phenomenon caused by a ballooning mode, which becomes unstable when the pressure gradient exceeds a critical value [9]. For the DIII-D tokamak discharge [9] ($I_p = 1.25$ MA, $B = 2.1$ T with assumption of $T_e = T_i$), the observed critical normalized pressure gradient prior to the occurrence of ELM is 0.11, higher than the maximum value achieved in LHD to date. In the LHD discharges, we have not seen any relaxation phenomena so far.

In smaller helical devices [4,5], edge transport barrier has been observed when the LCMS is close to the major rational surface. For the LHD configuration tested, the $\iota/2\pi$ surface is always located in the edge region where the pedestal exists. Thus the $\iota/2\pi$ surface or its associated island ($m/n = 1/1$) generated by error field may play some role in the formation of the edge thermal transport barrier.

In summary, we have achieved a significant improvement of the energy confinement with an edge thermal barrier in the LHD discharges. Key associated features of the LHD edge thermal barrier are quite different from those of H-mode discharges in tokamaks and helical devices and thus it is not any version of the H mode.

The authors thank Professor M. Fujiwara (director of NIFS) and Professor A. Iiyoshi (former director of NIFS) for their continuous guidance and encouragement.

[1] O. Motojima *et al.*, Phys. Plasmas **6**, 1843 (1999).
[2] F. Wagner *et al.*, Phys. Rev. Lett. **49**, 1408 (1982).
[3] K. Burrell *et al.*, Phys. Fluids B **2**, 1405 (1990).
[4] V. Erckmann *et al.*, Phys. Rev. Lett. **70**, 2086 (1993).
[5] K. Toi *et al.*, in *Plasma Physics and Controlled Nuclear Fusion Research 1992, Proceedings of the 14th Conference, Wurtzburg, 1992* (IAEA, Vienna, 1993), Vol. 2, p. 461.
[6] A. Fujisawa *et al.*, Phys. Rev. Lett. **82**, 2669 (1999).
[7] N. Ohyabu *et al.*, Nucl. Fusion **34**, 387 (1994).
[8] U. Stroth *et al.*, Nucl. Fusion **36**, 1063 (1996).
[9] P. Gohil *et al.*, Phys. Rev. Lett. **61**, 1603 (1988).